Structural Factors Contributing to the Hydrophobic Effect: The Partly Exposed Hydrophobic Minicore in Chymotrypsin Inhibitor 2†

Daniel E. Otzen,‡ Michael Rheinnecker,§ and Alan R. Fersht*

MRC Unit for Protein Function and Design and Cambridge Centre for Protein Engineering, Cambridge University Chemical Laboratory, Lensfield Road, Cambridge CB2 1EW, U.K.

Received May 23, 1995; Revised Manuscript Received August 3, 1995⊗

ABSTRACT: The structural basis for the stability of a partly solvent-exposed hydrophobic minicore, formed by the residues Leu51, Val57, and Phe69 in the reactive loop of the serine protease inhibitor chymotrypsin inhibitor 2 (CI2), was analyzed from the stability of 17 mutant proteins, in which side chain methylene groups were deleted or rearranged. The mutations destabilize the protein by 0.3−4.8 kcal/mol, an average of 0.6 kcal per removed methylene group. Double mutant cycles show significant interaction between individual pairs of side chains. There is an excellent linear correlation (r = 0.995) between the free energy of unfolding relative to wild type ($\Delta\Delta G_{U\text{-}F}$) and the packing density n_C (the number of methyl and methylene groups within 6 Å of the removed atoms). $\Delta\Delta G_{U\text{-}F}$ correlates more weakly with changes in solvent-accessible surface area upon mutation. The correlation improves when the change in solvent-accessible surface are upon mutation is separated into distinct contributions from polar atoms that are able to hydrogen bond to solvent (ΔA_{HB}) and from nonpolar atoms (ΔA_{HP}). There is also a correlation, however, between packing density and changes in surface area. Elsewhere in CI2, $\Delta\Delta G_{U\text{-}F}$ for mutations in the buried hydrophobic core correlates best with packing density, whereas in the exposed surface of the α-helix, the best correlation is with change in surface area. The results of hydrophobic changes at the surface of the protein are consistent with the classical model of the hydrophobic effect, whereas in the core, interactions are dominated by van der Waals' term, since van der Waals' interactions are additive; therefore, the higher the packing density, the stronger the van der Waals' interactions. The interdependence of the three structural parameters n_C, ΔA_{HP}, and ΔA_{HB} in the minicore suggests that interactions in partly exposed parts of proteins are governed by a mixture of the classical hydrophobic effect and van der Waals' interactions.

A continuing problem in current structural biology is quantifying the relative importance of different contributions to protein stability and elucidating their roles in protein folding. These contributions include the hydrophobic effect, hydrogen bonding, packing considerations (van der Waals' interactions), and electrostatic interactions. The hydrophobic effect was once considered simply in terms of the favorable entropy associated with the transfer of nonpolar amino acids from water into the predominantly nonpolar medium of the protein interior (Kauzmann, 1959; Tanford, 1973) but is increasingly being correlated with other structural features (Richards, 1977; Rose & Roy, 1980; Dill, 1990; Serrano et al., 1992a; Fersht & Serrano, 1993; Matthews, 1993). Protein engineering studies are now providing a wealth of data on noncovalent interactions in proteins. Detailed studies on a variety of proteins, such as barnase (Kellis et al., 1988, 1989), T4 lysozyme (Eriksson et al., 1993), chymotrypsin inhibitor 2 (Jackson et al., 1993), the λ repressor (Lim et al., 1992), bovine pancreatic trypsin inhibitor (Kim et al., 1993), staphylococcal nuclease (Shortle et al., 1990), and ribonuclease S (Varadarajan & Richards, 1992), have shown that the packing of nonpolar atoms and burial of hydrophobic surface area are the dominant forces in the stabilization of proteins. In the two major helices of barnase, changes in protein stability relative to wild type upon mutation ($\Delta\Delta G_{U\text{-}F}$)[1] correlate with the increased exposure of nonpolar surface area (Serrano et al., 1992b). However, a further term must be introduced when there are changes in the exposure of polar groups upon mutation (Serrano et al., 1992b). For buried residues, $\Delta\Delta G_{U\text{-}F}$ for mutations in the major hydrophobic cores of barnase (Serrano et al., 1992a) and chymotrypsin inhibitor 2 (Jackson et al., 1993) correlates with the packing density, that is, the number of methyl and methylene groups within a certain radius (6 Å) of the atoms removed by mutation. The packing density in protein interiors is higher than the packing density of small molecules in solution, implying a role for packing forces in protein stability (Harpaz et al., 1994b). $\Delta\Delta G_{U\text{-}F}$ has also been reported to correlate with the size of the cavity created by the truncation of hydrophobic side chains (Eriksson et al., 1992).

† D.E.O. is supported by a predoctoral fellowship from the Danish Natural Science Research Council. M.R. was supported by the Medical Research Council and Schering Agrochemicals Ltd.

* Author to whom correspondence should be addressed.

‡ Present address: Enzyme Function, Novo Nordisk A/S Novo Allé, DK-2880 Bagsvaerd, Denmark.

§ Present address: MorphoSys Gesellschaft für Proteinoptimierung mbH, Frankfurter Ring 193a, D-80807 Munich, Germany.

⊗ Abstract published in *Advance ACS Abstracts,* September 15, 1995.

[1] Abbreviations: CI2, chymotrypsin inhibitor 2; ΔA_{HP}, change upon mutation in solvent-accessible surface area of hydrophobic side chain atoms (methyl and methylene groups); ΔA_{HB}, change upon mutation in solvent-accessible surface area of polar atoms (carbonyl O and NH) that do not make internal hydrogen bonds; $\Delta\Delta G_{U\text{-}F}$, free energy of unfolding relative to wild type CI2; $\Delta\Delta G_{int}$, coupling energy between specific residues; F, folded state; GdmCl, guanidine hydrochloride; n_C, packing density = the number of methyl or methylene groups within a sphere of radius 6 Å from the center of a particular atom; r, correlation coefficient; U, unfolded state.

0006-2960/95/0434-13051$09.00/0

Most of the work on the hydrophobic effect has concentrated on protein cores, which are formed from the burial and interdigitation of hydrophobic side chains from secondary structure elements such as β-sheets and α-helices. The magnitude of the hydrophobic effect in small hydrophobic patches is not known. These patches, which we call hydrophobic minicores, are tertiary structures formed by small clusters of hydrophobic side chains that are partly exposed to solvent.

The protein chymotrypsin inhibitor 2 (CI2) is an attractive model for stability studies. Its structure is known both in the crystal form (Harpaz et al., 1994a; McPhalen & James, 1987) and in solution (Ludvigsen et al., 1991). It belongs to a family of serine protease inhibitors, which do not have cysteine residues, and where disulfide bridges that are formed in other families have been replaced by electrostatic and hydrophobic interactions stabilizing the exposed reactive site loop (Bode & Huber, 1992). CI2 has been shown to fold according to a two-state system between the unfolded and the native state under both equilibrium and nonequilibrium conditions (Jackson & Fersht, 1991).

In this report, we present results of a study on a hydrophobic minicore in CI2. The minicore consists of three conserved residues, namely Leu51, Val57, and Phe69, whose side chains interact extensively to bury a large amount of hydrophobic surface area. In contrast to residues in the major core of CI2, the side chains remain partly exposed to solvent. This enables us to examine the correlation between changes in solvent-accessible surface area, as well as packing density, and changes in stability resulting from the removal of methyl(ene) groups. The accurate and predictive analysis of energetic consequences of such mutations is beyond present capabilities in computational procedures. We are just seeking simple statistical correlations between the energies and easily measurable physical properties. The properties found most useful so far are as follows: n_C, the number of methyl or methylene groups surrounding a methyl(ene) group that is removed by mutation (empirically, within a sphere of radius 6 Å from its center) (Serrano et al., 1992a); ΔA_{HP}, the change upon mutation in solvent-accessible surface area of hydrophobic side chain atoms in the protein (Serrano et al., 1992b); and ΔA_{HB}, the change upon mutation in solvent-accessible area of polar atoms in the protein that can form hydrogen bonds to solvent molecules (Serrano et al., 1992b).

EXPERIMENTAL PROCEDURES

Materials. All chemicals were obtained as described (Jackson et al., 1993). In addition, recombinant *Pfu* DNA polymerase with reaction buffer 3 was obtained from Stratagene, USBioclean kit from United States Biochemical, and single-stranded DNA purification kits from Clontech and Promega.

Preparation of Mutants. Naturally occurring CI2 is an 83-residue protein, where the first 19 residues do not have fixed structure. A truncated version lacking these first 19 residues has been constructed (Jackson et al., 1993). This truncation does not affect its biological properties and has no significant effect on the kinetics and thermodynamics of folding. The gene for a truncated version of CI2 (Met20-Gly83), lacking the first 19 amino acids, has been cloned into a pTZ18U vector downstream of a T7 Φ-promoter and ribosome binding site (Jackson et al., 1993). Site-directed mutagenesis on this gene was carried out by inverse PCR (Innis & Gelfand, 1990). For each mutation, two 36-nucleotide primers were constructed, one from the coding strand of plasmid, the other from the complementary strand. The mutagenic primer, usually based on the coding strand, had the mutated codon placed at its 5′-end, followed by the 11 codons downstream of the site of mutation in the gene sequence. The noncoding primer was composed of the sequence complementary to the 12 codons immediately upstream from the site of mutation. Each primer was 5′-phosphorylated by incubation of 10 μM primer for 1 h at 37 °C in a volume of 40 μL with 5 units of T4 polynucleotide kinase in 1 mM ATP, 10 mM DTT, 50 mM Tris-HCl (pH 7.5), 10 mM $MgCl_2$, 0.1 mM spermidine chloride, and 0.1 mM EDTA (pH 8.0). Following heat inactivation of the kinase (5 min at 95 °C), 1.5 μL of both primer solutions was incubated in a 50 μL reaction volume with 0.2 mM dNTPs, 3 units of recombinant *Pfu* DNA polymerase, 5 μL of a 1:100 dilution of a single-stranded DNA preparation of the CI2 template (prepared using the glass-phage kit from Clontech or the Wizard M13 DNA purification system from Promega), 20 mM Tris-HCl (pH 7.5), 8 mM $MgCl_2$, and 400 μg/mL BSA. The following temperature cycles were then carried out: 4 min at 94 °C, followed by 25 cycles of 1 min at 94 °C, 1 min at 55 °C, and 7 min at 72 °C. Single-stranded DNA was visualized in 2% agarose gels, isolated using the USBioclean kit from United States Biochemical, and ligated in a 10 μL reaction volume with 5 units of T4 DNA ligase in 100 mM Tris-HCl (pH 7.6) and 5 mM $MgCl_2$ before transformation. Mutants were identified by the direct sequencing of the single-stranded DNA. Expression and purification were performed as described (Jackson et al., 1993).

Analysis of Protein Stability. Equilibrium denaturation with guanidinium chloride (GdmCl) and data analysis were carried out as described (Jackson et al., 1993). In brief, aliquots of increasing concentrations of GdmCl in 50 mM MES (pH 6.25) were prepared and incubated at 25 °C with ca. 2 μM protein for at least 1 h before the fluorescence emission at 356 nm on excitation at 280 nm was measured. The plot of fluorescence intensity versus GdmCl concentration was fitted to the following two-state equation (Clarke & Fersht, 1993) using the program KaleidaGraph:

$$F = [(\alpha_N + \beta_N[\mathrm{GdmCl}]) + (\alpha_U + \beta_U[\mathrm{GdmCl}]) \exp[m_{U\text{-}F}([\mathrm{GdmCl}] - [\mathrm{GdmCl}]^{50\%})/RT]]/[1 + \exp[m_{U\text{-}F}([\mathrm{GdmCl}] - [\mathrm{GdmCl}]^{50\%})/RT]] \quad (1)$$

where F is the measured fluorescence, α_N and α_U are the intercepts and β_N and β_U are the slopes of the fluorescence base lines at low (N) and high (U) GdmCl concentrations before and after the transition region of unfolding, $[\mathrm{GdmCl}]^{50\%}$ is the concentration of GdmCl at which the protein is 50% denatured, and $m_{U\text{-}F}$ is a constant from the following equation (Tanford, 1968):

$$\Delta G_{U\text{-}F}{}^{D} = \Delta G_{U\text{-}F}{}^{H_2O} - m_{U\text{-}F}[\mathrm{GdmCl}] \quad (2)$$

where $\Delta G_{U\text{-}F}{}^{D}$ is the free energy of unfolding of proteins in the presence of GdmCl and $\Delta G_{U\text{-}F}{}^{H_2O}$ is the free energy of unfolding in water.

Table 1: Sequence Comparisons in the Hydrophobic Minicore of CI2 with Homologous Proteins[a]

protein	residue 51	residue 57	residue 69
CI2	Val	Val	Phe
CI1	Val	Val	Leu
eglin *c*	Phe	Val	Phe
potato inhibitor 1	Ile	Val	Phe
yeast protease B inhibitor	Ile	Val	Lys

[a] From Svendsen et al. (1982).

$\Delta\Delta G_{U\text{-}F}^{[G]50\%}$, the difference in stability between wild type and mutant CI2 at a mean value of $[GdmCl]^{50\%}$ for the two proteins, is calculated as

$$\Delta\Delta G_{U\text{-}F}^{[G]50\%} = \langle m_{U\text{-}F}\rangle \Delta[GdmCl]^{50\%} \quad (3)$$

where $\langle m_{U\text{-}F}\rangle$ is the average value of $m_{U\text{-}F}$ for a large number of CI2 mutants (1.94 ± 0.025 kcal mol^{-2}) and $\Delta[GdmCl]^{50\%}$ is the difference in $[GdmCl]^{50\%}$ between the wild type and mutant CI2. Shorter extrapolation means that $\Delta\Delta G_{U\text{-}F}^{[G]50\%}$ has a smaller standard error than the difference in stability between wild type and mutant CI2 in water ($\Delta\Delta G_{U\text{-}F}^{H_2O}$) (Jackson et al., 1993). We shall refer to $\Delta\Delta G_{U\text{-}F}^{[G]50\%}$ as $\Delta\Delta G_{U\text{-}F}$ throughout.

Surface Area Calculations. Structural analysis was based on the crystal structure of the double mutant Glu→Ala33/Glu→Ala34 (which we call the pseudo-wild type) (Harpaz et al., 1994a) which has been solved to higher resolution than that of the wild type (McPhalen & James, 1987). For each mutant protein, appropriate atoms in the coordinate file of the pseudo-wild type crystal structure were deleted, and solvent-accessible surface area was calculated using a program based on an algorithm employing a rolling sphere of radius 1.4 Å (Y. Harpaz, Centre for Protein Engineering, Cambridge), similar to that of Lee and Richards (1971). Differences in surface area between wild type and mutant were calculated as follows. For each atom of the protein with a surface area altered by the mutation, the area difference ΔA (in Å^2) between the mutant and wild type was calculated by subtraction of the area of the atom in the mutant atom from the area of the corresponding atom in the wild type. Values of ΔA for all methyl(ene) carbon atoms in the protein, i.e. all carbon atoms except the carbonyl carbon, were summed to give the change in solvent-accessible hydrophobic surface area (ΔA_{HP}). Similarly, summing the values of ΔA for all carbonyl oxygen atoms and amide nitrogen atoms that do not form hydrogen bonds internally in the protein gives the change in solvent-accessible surface area of polar atoms which require solvation (ΔA_{HB}) (Serrano et al., 1992b).

Packing Density. For each mutant, the packing density was empirically determined as the number of methyl or methylene groups within 6 Å of any side chain atom removed by mutation. For double and triple mutants, where atoms from two or more side chains were removed, atoms removed from one mutated side chain, which in the pseudo-wild type structure are within 6 Å of atoms removed from another mutated side chain, were not counted.

Inhibitory Studies. Studies on the inhibition of subtilisin by mutants of CI2 were carried out as described (Longstaff et al., 1990), with the modification that all data were collected with a cycle time of 60 s. Subtilisin BPN′ (250 pM) was incubated with 1 mM substrate (succinyl-Ala-Pro-Phe-*p*-succinylanilide) in 10 mM Tris-HCl (pH 8.6) at 25 °C and different concentrations of CI2 (2.5−15 nM). The rate of hydrolysis was followed by monitoring the absorbance at 412 nm. The reaction was monitored for at least 20 half-lives of the binding reaction. Data were analyzed using the program KaleidaGraph and rate equations describing substrate hydrolysis in the presence of slow-binding inhibitor (Longstaff et al., 1990). We obtain the energy of binding of CI2 to subtilisin relative to wild type ($\Delta\Delta G_{binding}$) from the inhibition constant K_i:

$$\Delta\Delta G_{binding} = -RT \ln(K_i^{mutant}/K_i^{wild\ type}) \quad (4)$$

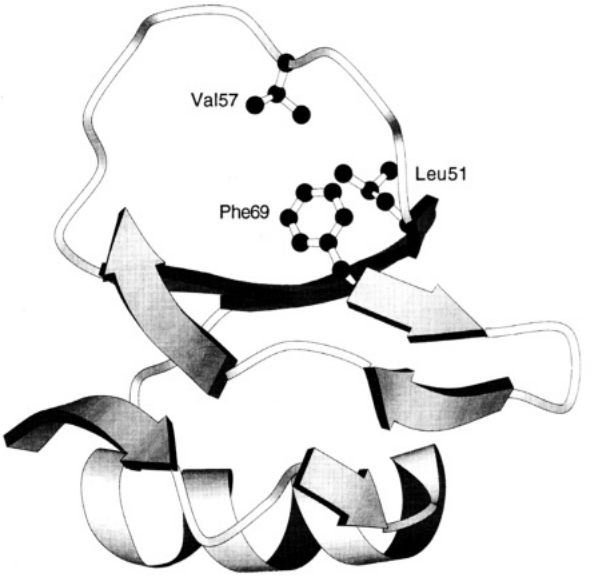

FIGURE 1: Schematic representation of the side chain interactions in the hydrophobic minicore of CI2, consisting of residues Leu51, Val57, and Phe69 [using the program Molscript (Kraulis, 1991) and the Brookhaven file 2CI2].

RESULTS

Description of Mutated Residues. The hydrophobic minicore is very well-conserved in the family of inhibitors to which CI2 belongs (Table 1). Residue 51 is always hydrophobic, residue 57 always Val, and residue 69 always large and hydrophobic, apart from there being a lysine in the yeast protease B inhibitor, which does have a hydrophobic region in its side chain. The side chains interact extensively, forming a well-defined minicore (Figure 1).

Residues 52 (Pro) and 55 (Thr), though close to the patch, are not conserved to a similar degree (Svendsen et al., 1982) and contribute little to the stability of CI2. The mutations Pro→Ala52 and Thr→Ala55 destabilize the protein by less than 0.3 kcal/mol (D. E. Otzen, L. S. Itzhaki, and A. R. Fersht, unpublished results). Arg67 is the only residue whose side chain is within 4.5 Å of all three minicore residues. The methylene groups of this Arg67 are, therefore, close enough to the minicore residues for hydrophobic contact. Removal of the arginine side chain by mutation to alanine destabilizes the protein by 1.2 kcal/mol, while replacement by cysteine actually stabilizes it by 0.3 kcal/mol (D. E. Otzen and A. R. Fersht, unpublished results).

The minicore side chains are not completely buried (Table 2). This enables us to calculate changes in solvent-accessible surface area upon mutation. There is extensive packing of

Table 2: Solvent Exposure of Side Chains (C^{γ} Outward) and Side Chain Interactions with 4.5 Å in the Minicore

residue	no. of methyl(ene) groups within 6 Å of side chain atoms (C^{γ} outward)	*B* factors	solvent exposure, (Å^2)	side chains within 4.5 Å
Leu 51	47	C^{β}: 9.7 C^{γ}: 10.7 C^{δ}: 12.6 $C^{\delta 2}$: 11.0	42	I49, V50, P52, T55, V57, R67, L68, F69
Val 57	25	C^{β}: 14.7 $C^{\gamma 1}$: 14.5 $C^{\gamma 2}$: 14.2	33	L51, T55, I56, T58, R67, F69
Phe 69	94	C^{β}: 7.9 C^{γ}: 9.1 $C^{\delta 1}$: 9.0 $C^{\delta 2}$: 9.5 $C^{\epsilon 1}$: 9.9 $C^{\epsilon 2}$: 10.5 C^{ξ}: 9.8	31	L51, P52, V53, V57, R67, L68, V70, E78

methylene groups around each side chain (Table 2). The *B* factors from the crystal structure, which indicate the spatial or temporal confinement of each atom in the structure, are all below 15 Å^2 (Table 2). Thus, the positions of the side chain atoms are all well-defined.

Equilibrium Denaturation. The use of GdmCl denaturation experiments to determine the stability of CI2 mutants has been discussed in detail (Jackson et al., 1993). There are large individual variations in $m_{U\text{-}F}$, the parameter which measures the dependence of $\Delta G_{U\text{-}F}$, the free energy of unfolding of the protein, on GdmCl-concentration (eq 2). The values range from 1.59 ± 0.14 to 2.37 ± 0.13 (Table 3). The average value of $m_{U\text{-}F}$ is 1.98 ± 0.05, which is identical within error to that of wild type CI2 (1.90 ± 0.03) and close to the average value of $m_{U\text{-}F}$ for all CI2 mutants prepared and characterized so far (1.94 ± 0.025). We have used the average $m_{U\text{-}F}$ value for calculating $\Delta\Delta G_{U\text{-}F}^{[GdmCl]50\%}$, the value of $\Delta\Delta G_{U\text{-}F}$ at a GdmCl concentration midway between the concentrations at which 50% of the mutant and wild type are denatured (eq 3). This $\Delta\Delta G_{U\text{-}F}$ value gives a lower error than $\Delta\Delta G_{U\text{-}F}$ in water due to shorter extrapolation (Table 3) and was previously shown to be identical, within 1−2%, to $\Delta\Delta G_{U\text{-}F}$ derived from differential-scanning calorimetry (Jackson et al., 1993) [it has been argued elsewhere (Serrano et al., 1992a) that the large variation in individual values of $m_{U\text{-}F}$ for mutants of proteins that do not accumulate folding intermediates results from experimental error and that the true values are close to the mean of many measurements].[2]

The observed values of $\Delta\Delta G_{U\text{-}F}$ span 4.5 kcal/mol, from 0.25 kcal/mol (the mutation Leu→Ile51, which involves only a switch in the position of one methyl group) to 4.79 kcal/mol (the double mutation Leu→Ala51/Phe→Ala69 which removes nine methyl(ene) groups). The penalty for removing a methylene group thus varies from 0.44 to 0.79 kcal/mol, with an average of 0.59 ± 0.03. This value is well below that seen for mutations in the hydrophobic core of CI2, where the average change in $\Delta\Delta G_{U\text{-}F}$ per methyl group deleted is 1.3 ± 0.5 kcal/mol. However, in the latter case, the mutated residues are almost all completely buried.

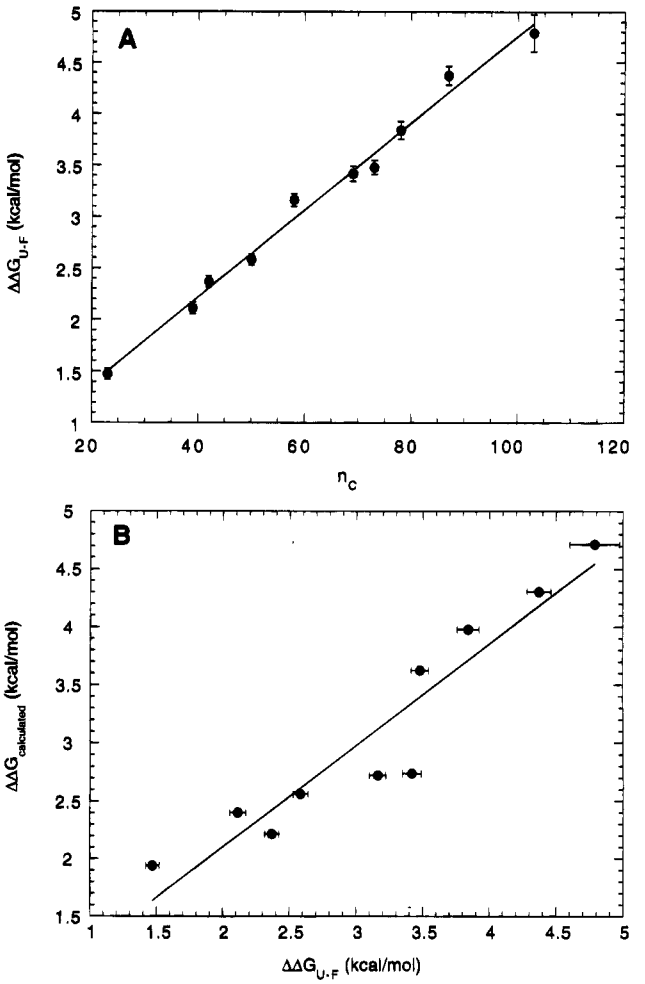

FIGURE 2: Correlation of packing density and changes in surface area with stability changes for mutations in the minicore. (A) Packing density (i.e. the number of methyl(ene) groups within 6 Å of the atoms removed by mutation) and $\Delta\Delta G_{U\text{-}F}$. A linear fit to the 10 points yields a line of slope 0.042 ± 0.002 and a correlation coefficient r = 0.995. (B) $\Delta\Delta G_{calculated}$ (from a multiple linear regression analysis incorporating ΔA_{HP} and ΔA_{HB}) versus $\Delta\Delta G_{U\text{-}F}$. The 10 points are fitted to a line of slope 0.90 ± 0.11 and an intercept of 0.33 ± 0.36, giving a correlation coefficient r = 0.95.

Correlation of Stability Changes with Packing Density and Changes in Solvent-Accessible Surface Area. Only 10 of the 17 minicore mutants could be modeled simply by deletion of methyl(ene) groups for calculation of changes in solvent-accessible surface area. The other seven mutants involve changes in stereochemistry (e.g. Leu→Val51 and Phe→Val69). These mutants could not be constructed from the wild type crystal or solution structures. Similar restrictions apply to the analysis of packing changes, where the number of methyl(ene) groups within 6 Å of the atoms removed by mutation is counted.

There is an excellent linear relationship between $\Delta\Delta G_{U\text{-}F}$ and packing density for the 10 mutants (Figure 2A). A linear fit gives the following equation (standard errors in brackets):

$$\Delta\Delta G_{U\text{-}F} = 0.53 \pm 0.10 + (0.042 \pm 0.002)n_C \quad \text{(kcal/mol)} \quad (r = 0.995 \text{ for 10 points}) \quad (5)$$

[2] A referee has asked us to comment on the wide variation of *m* values found for staphylococcal nuclease. Creighton and Shortle (1994) have now found that there is a compact folding intermediate present under the denaturing conditions used for determination of *m* for this protein and so the earlier values were not derived under conditions for a two-state transition, as inferred from the arguments of Serrano et al. (1992a).

Table 3: Equilibrium Denaturation Data for Mutants in the Minicore[a]

mutant	$m_{U\text{-}F}$	$[GdmCl]^{50\%}$	$\Delta\Delta G_{U\text{-}F}$ (kcal/mol)	no. of CH groups removed	$\Delta\Delta G_{U\text{-}F}$ per methylene group (kcal/mol)
wild type	1.90 ± 0.03	4.00 ± 0.01	0	–	–
LA51	2.11 ± 0.10	2.78 ± 0.02	2.37 ± 0.05	3	0.79 ± 0.02
LI51	1.70 ± 0.08	3.87 ± 0.03	0.25 ± 0.07	0	–
LV51	1.76 ± 0.09	3.74 ± 0.03	0.50 ± 0.06	1	0.50 ± 0.06
LV51/FL69	2.37 ± 0.13	2.75 ± 0.02	2.42 ± 0.06	4	0.61 ± 0.02
LV51/FA69	1.94 ± 0.09	2.24 ± 0.02	3.41 ± 0.07	7	0.46 ± 0.01
LA51/FL69	1.94 ± 0.08	2.24 ± 0.02	3.42 ± 0.07	6	0.57 ± 0.01
LA51/FA69	1.59 ± 0.14	1.53 ± 0.08	4.79 ± 0.19	9	0.53 ± 0.02
LA51/VA57	1.96 ± 0.06	2.37 ± 0.01	3.16 ± 0.06	5	0.53 ± 0.01
LV51/VA57	1.86 ± 0.06	3.05 ± 0.01	1.85 ± 0.05	3	0.62 ± 0.02
LA51/VA57/FL69	1.93 ± 0.06	2.21 ± 0.01	3.48 ± 0.07	8	0.44 ± 0.01
LV51/VA57/FL69	1.83 ± 0.05	2.60 ± 0.01	2.72 ± 0.05	6	0.45 ± 0.01
VA57	2.14 ± 0.12	3.24 ± 0.02	1.47 ± 0.05	2	0.73 ± 0.03
VA57/FL69	2.02 ± 0.08	2.67 ± 0.01	2.58 ± 0.06	5	0.52 ± 0.01
VA57/FA69	2.19 ± 0.12	1.75 ± 0.02	4.37 ± 0.09	8	0.55 ± 0.01
FL69	1.95 ± 0.11	2.91 ± 0.02	2.11 ± 0.06	3	0.74 ± 0.02
FV69	2.24 ± 0.18	2.77 ± 0.03	2.39 ± 0.07	4	0.60 ± 0.02
FA69	2.17 ± 0.13	2.02 ± 0.03	3.84 ± 0.08	6	0.64 ± 0.01

[a] All measurements were carried out at 25 °C and pH 6.25.

where n_C is the number of methyl or methylene groups within a sphere of radius 6 Å from the center of each methylene group deleted by mutation and r is the correlation coefficient. A similar analysis, in which all atoms (not just methyl and methylene groups) within 6 Å of the mutated atoms were counted, also gives a very good correlation, in which the slope is 0.018 ± 0.001 and $r = 0.98$.

There is a more modest correlation between $\Delta\Delta G_{U\text{-}F}$ and the change in exposed hydrophobic surface area (ΔA_{HP}) for these 10 minicore mutants:

$$\Delta\Delta G_{U\text{-}F} = 3.0 \pm 0.3 - (0.059 \pm 0.021)\Delta A_{HP} \quad \text{(kcal/mol)} \quad (6)$$

($r = 0.71$ for 10 points, which is significant at the 98% confidence limit). A similar plot of the change in exposed surface area of polar atoms which can form hydrogen bonds to solvent molecules (ΔA_{HB}) gives a correlation coefficient of 0.82 (10 points). However, the expression of $\Delta\Delta G_{U\text{-}F}$ versus a combination of ΔA_{HB} and ΔA_{HP}, using a multiple linear regression analysis, yields the equation

$$\Delta\Delta G_{U\text{-}F} = 1.78 \pm 0.26 - (0.041 \pm 0.011)\Delta A_{HP} + (0.06 \pm 0.01)\Delta A_{HB} \quad \text{(kcal/mol)} \quad (7)$$

This equation is similar to one derived from analysis of a series of Ala→Gly mutations in the two major helices of the ribonuclease barnase from *Bacillus amyloliquefaciens* (Serrano et al., 1992b), namely

$$\Delta\Delta G_{Gly\rightarrow Ala} = 1.59 \pm 0.24 - (0.041 \pm 0.013)\Delta A_{HP} + (0.19 \pm 0.03)\Delta A_{HB} \quad \text{(kcal/mol)} \quad (8)$$

ΔA_{HP} and ΔA_{HB} are approximately the same magnitude in eq 7 but have different signs. An increase in the solvent-accessible surface area of polar atoms able to make hydrogen bonds to water (i.e. $\Delta A_{HB} < 0$) is favorable, since it satisfies the hydrogen bond requirements of otherwise unpaired polar atoms in the protein. Conversely, increasing the solvent-accessible surface area of nonpolar atoms (i.e. $\Delta A_{HP} < 0$) is entropically unfavorable.

A plot of $\Delta\Delta G_{calculated}$ from eq 7 against the value of $\Delta\Delta G_{U\text{-}F}$ measured for each mutant (Figure 2B) fits to the line

$$\Delta\Delta G_{calculated} = 0.33 \pm 0.36 + (0.90 \pm 0.11)\Delta\Delta G_{U\text{-}F} \quad (r = 0.95 \text{ for 10 points}) \quad (9)$$

Why, then, is $\Delta\Delta G_{U\text{-}F}$ correlated both with n_C (eq 5) and with ΔA_{HP} (eq 6) and ΔA_{HB}? The better correlation is with n_C, and there is a poorer correlation with ΔA_{HP} and ΔA_{HB}. We find correlations between n_C and both ΔA_{HP} and ΔA_{HB} for this partly exposed core that account for the dual correlation:

$$\Delta A_{HP} = 20.2 \pm 4 - (0.38 \pm 0.12)n_c \quad (r = 0.74 \text{ for 10 points}) \quad (10)$$

$$\Delta A_{HB} = 2.8 \pm 6.4 - (0.37 \pm 0.10)n_c \quad (r = 0.80 \text{ for 10 points}) \quad (11)$$

In the main hydrophobic core of CI2 that is almost completely buried, the correlation is clearly between $\Delta\Delta G_{U\text{-}F}$ and n_C (Jackson et al., 1993).

Comparison with Other Hydrophobic Mutations in CI2. Mutations involving only deletions of methyl(ene) groups have been carried out in other parts of CI2 in addition to the minicore, namely in the main hydrophobic core (Jackson et al., 1993), the α-helix (L. S. Itzhaki and A. R. Fersht, unpublished data), and the β-sheet (Otzen & Fersht, 1995), comprising in all 47 different deletions. The minicore clearly yields the best correlations between changes in stability and changes in solvent-accessible surrface area and packing density. When all 47 mutants are considered together, the correlation between $\Delta\Delta G_{U\text{-}F}$ and n_C is as follows (Figure 3):

$$\Delta\Delta G_{U\text{-}F} = 0.17 \pm 0.18 + (0.050 \pm 0.004)n_c \quad (r = 0.86 \text{ for 47 points}) \quad (12)$$

A similar analysis of mutations in the cores of barnase has been carried out (Serrano et al., 1992a), yielding the correlation

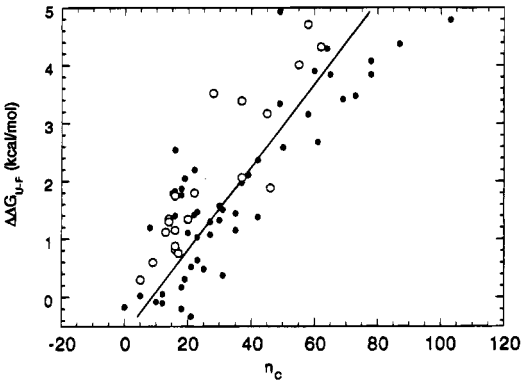

FIGURE 3: Correlation of packing density and changes in surface area with stability changes for 47 hydrophobic mutations in CI2 (filled circles). A linear fit gives a line of slope 0.05 ± 0.004 with correlation coefficient $r = 0.86$ (47 points). Similar data obtained from barnase are shown in open circles.

$$\Delta\Delta G_{U\text{-}F} = 0.13 \pm 0.25 + (0.069 \pm 0.008)n_C \quad (r = 0.90 \text{ for 20 points}) \quad (13)$$

The slope is similar to that obtained for the core of CI2 (0.072 ± 0.012). The minicore has a smaller slope (0.042 ± 0.004). Comparison of n_C for similar classes of mutation (both Val→Ala and Leu→Ala) in the major core and minicore of CI2 show that the core is ca. 1.5 times more tightly packed than the more surface-exposed hydrophobic minicore. However, the packing density in the major hydrophobic core of barnase is very similar to that of the minicore. For all 47 hydrophobic mutations in CI2, the correlation between $\Delta\Delta G_{U\text{-}F}$ and ΔA_{HP} is

$$\Delta\Delta G_{U\text{-}F} = 2.14 \pm 0.17 - (0.058 \pm 0.011)\Delta A_{HP} \quad (r = 0.62 \text{ for 47 points}) \quad (14)$$

The best correlation between $\Delta\Delta G_{calculated}$ and $\Delta\Delta G_{U\text{-}F}$ for all the mutants is obtained by performance of a multiple linear regression analysis on a combination of the core and minicore data. This still yields a poor correlation. By themselves, ΔA_{HP} and ΔA_{HB} also lead to a poor correlation between $\Delta\Delta G_{U\text{-}F}$ and $\Delta\Delta G_{calculated}$ after multiple linear regression analysis is performed on all 47 CI2 mutants. All this reinforces the conclusion that packing density is the most significant contributor to protein stability in regions of tertiary structure. However, in elements of secondary structure, this is not the case. Stability changes in the major helices of barnase correlate very well with increased exposure of nonpolar and polar surface area (Serrano et al., 1992b), but not with packing ($r = 0.3$ for 12 points, which is below the 90% confidence limit). Packing is not observed to correlate with stability changes in the β-sheet of CI2 (Otzen & Fersht, 1995) or the α-helix of CI2 (L. S. Itzhaki and A. R. Fersht, unpublished results).

Inhibition Studies. Mutations in the minicore cause no dramatic changes in the ability of CI2 to inhibit the proteolytic activity of subtilisin. $\Delta\Delta G_{binding}$ relative to wild type (eq 4) is in all cases less than 1 kcal/mol (Table 4). For comparison, the mutation Thr→Asp58 in the residue before the scissile bond between Met59 and Glu60 results in a $\Delta\Delta G_{binding}$ of 2.1 ± 0.10 kcal/mol (Jackson & Fersht, 1994). The side chain of Val57 makes no direct contacts with subtilisin, and Phe69 is completely outside the region of contact with subtilisin (McPhalen et al., 1985). The backbone of Leu51 does not make any hydrogen bonds with subtilisin.

Table 4: Inhibitory Activity of Various Minicore Mutants[a]

mutant	k_{on} (10^6 s^{-1} M^{-1})	k_{off} (10^{-6} s^{-1})	K_i (10^{-12} M)	$\Delta\Delta G_{binding}$ (kcal/mol)
wild type	3.14 ± 0.33	6.13 ± 0.99	1.95 ± 0.24	0
LA51	5.83 ± 0.06	39.74 ± 4.16	6.81 ± 0.10	0.74 ± 0.09
VA57	3.90 ± 0.21	15.65 ± 1.67	4.01 ± 0.37	0.43 ± 0.05
VA57/FA69	6.34 ± 1.25	23.70 ± 6.63	3.74 ± 0.74	0.38 ± 0.05
FA69	3.75 ± 0.23	20.97 ± 3.60	5.59 ± 0.89	0.62 ± 0.08

[a] Measured from the inhibition of subtilisin BPN′ by CI2 at 25 °C and pH 8.6 (see Experimental Procedures for details).

Table 5: Interaction Energies in the Minicore of CI2

double mutant	$\Delta\Delta G_{int}^{U\text{-}F}$ (water)[a] (kcal/mol)	$\Delta\Delta G_{U\text{-}F}$[b] (kcal/mol)	$(\Delta\Delta G_{int}^{U\text{-}F})/(\Delta\Delta G_{U\text{-}F}^{[G]50\%})$
LV51/FL69	0.19 ± 0.03	2.42 ± 0.06	0.08
LV51/FA69	0.93 ± 0.04	3.41 ± 0.07	0.27
LA51/FL69	1.06 ± 0.04	3.42 ± 0.07	0.31
LA51/FA69	1.42 ± 0.07	4.79 ± 0.19	0.30
VA57/FL69	1.00 ± 0.03	2.58 ± 0.06	0.39
VA57/FA69	0.94 ± 0.04	4.37 ± 0.09	0.22
LA51/VA57	0.68 ± 0.10	3.16 ± 0.06	0.22
LV51/VA57	0.13 ± 0.09	1.85 ± 0.05	0.07

[a] For double mutant analysis of residues X and Y, $\Delta\Delta G_{int}^{U\text{-}F} = \Delta\Delta G_{E\text{-}XY\rightarrow E\text{-}Y}^{U\text{-}F} + \Delta\Delta G_{E\text{-}XY\rightarrow E\text{-}X}^{U\text{-}F} - \Delta\Delta G_{E\text{-}XY\rightarrow E}^{U\text{-}F}$. [b] The energy term from Table 3 ≡ $\Delta\Delta G_{E\text{-}XY\rightarrow E}^{U\text{-}F}$.

Double and Triple Mutant Cycles. Values of $\Delta\Delta G_{U\text{-}F}$ obtained from individual mutants measure the effect of the mutation on the overall stability of the protein. These effects are the sum of many individual interactions and involve all atoms directly or indirectly affected by the removal or rearrangement of methyl(ene) groups. However, it is possible to focus specifically on the interaction between two or three residues by performance of double or triple mutant cycles. The rationale for this approach has been discussed (Fersht et al., 1990). Ideally, multiple mutant cycles cancel out all interactions except those between the residues mutated in the cycle. The coupling energy $\Delta\Delta G_{int}$ between two residues X and Y is calculated from

$$\Delta\Delta G_{int} = \Delta\Delta G_{E\text{-}X} + \Delta\Delta G_{E\text{-}Y} - \Delta\Delta G_{E\text{-}XY} \quad (15)$$

where $\Delta\Delta G_{E\text{-}XY}$ is the change in stability (relative to wild type) of the mutant where both X and Y are mutated and $\Delta\Delta G_{E\text{-}X}$ and $\Delta\Delta G_{E\text{-}Y}$ are the changes in stability of the mutants where X and Y, respectively, are mutated. The coupling energies involving the three side chains in the minicore generally contribute a substantial part of the overall destabilization energy (Table 5), showing that there is synergy in the minicore, almost certainly resulting from direct pairwise interactions. Mutations involving Leu→Val51 are an exception; values of $\Delta\Delta G_{int}$ are very low, unless the phenylalanine ring of Phe69 is completely truncated to Ala.

Values of $\Delta\Delta G_{U\text{-}F}$ for triple mutants allow us to expand to higher-order interaction energies encompassing all three residues. The value of $\Delta^3 G_{int}$ for a given triple mutant is a measure of the coupling between all three residues, i.e. the difference between the destabilization of the triple mutant and the sum of the pairwise interaction energies and the destabilization energies of the individual mutants (Horovitz & Fersht, 1992):

$$\Delta^3G_{int}^{U\text{-}F} = \Delta\Delta G_{E\text{-}XYZ\rightarrow E}^{U\text{-}F} - \Delta\Delta G_{E\text{-}XYZ\rightarrow E\text{-}X}^{U\text{-}F} + \Delta\Delta G_{E\text{-}XYZ\rightarrow E\text{-}Y}^{U\text{-}F} + \Delta\Delta G_{E\text{-}XYZ\rightarrow E\text{-}Z}^{U\text{-}F} + \Delta\Delta G_{E\text{-}XYZ\rightarrow E\text{-}YZ}^{U\text{-}F} + \Delta\Delta G_{E\text{-}XYZ\rightarrow E\text{-}XZ}^{U\text{-}F} + \Delta\Delta G_{E\text{-}XY\rightarrow E\text{-}XY}^{U\text{-}F} \quad (16)$$

This corresponds to measurement of the difference in $\Delta\Delta G_{int}$ for cycles at opposite faces of a triple mutant box (Figure 4). In physical terms, Δ^3G_{int} is the change in pairwise interaction energies upon the addition of the third residue.

The triple mutant Leu→Ala51/Val→Ala57/Phe→Val69 has a Δ^3G_{int} value of 0.27 ± 0.16 kcal/mol (Table 6). Similarly, Δ^3G_{int} for the mutant Leu→Val51/Val→Ala57/Phe→Val69 is close to 0. Thus, the energy of forming the minicore is equal to the sum of its pairwise interactions and there is no additional synergy of having all three side chains present.

DISCUSSION

In this study, we report a detailed analysis of a series of mutations of the three-residue minicore in CI2 consisting of Leu51, Val57, and Phe 69. The residues form a cluster of nonpolar atoms outside the main hydrophobic core of the protein. The structure of the minicore is stabilized by hydrophobic interactions alone; no hydrogen bonding between backbone atoms is involved. The 17 mutations destabilize the protein by between 0.3 and 4.8 kcal/mol and provide a convenient system with which to examine the effects of different structural parameters on protein stability and folding over a wide range of free energy. Further, the mutations do not significantly affect the inhibitory properties of the protein. Loss of inhibitory activity would indicate significant structural rearrangement, since the side chains of the minicore in the wild-type structure do not interact extensively with the protease subtilisin BPN′ (McPhalen et al., 1985). The destabilization of the minicore by mutations results in part from the loss of interactions between the minicore residues, since double mutant cycles demonstrate a coupling energy $\Delta\Delta G_{int}$ between the residues of up to 40% of the overall destabilization energy $\Delta\Delta G_{U\text{-}F}$ (Table 5). The pairwise interactions between the residues are not appreciably affected by the presence of the third side chain, since Δ^3G_{int} is close to 0.

The mutations remove interactions without introducing new ones (except in the case of the Leu→Ile51 mutant). They involve the removal of up to nine methylene groups per mutation, giving an average loss in stability of 0.59 ± 0.03 kcal per methylene group. This is less than that observed for the major hydrophobic core of CI2, which is formed by one side of the α-helix docking onto the β-sheet, where the mean loss in stability is 1.3 kcal per methylene group (Jackson et al., 1993). The side chains of the minicore are less well-buried than those in the core.

Mutations can affect the stability of the unfolded state as well as the folded state. Therefore, when mutations involving replacement of different amino acids (which will have different solvent interactions in the unfolded state) are compared, surface area changes in the unfolded state should in principle be included. However, molecular dynamics simulations (Prevost et al., 1991) have shown that the effect of mutation on protein stability predominantly arises from the difference in stability of the folded rather than the unfolded state. These findings are supported by our ability to correlate $\Delta\Delta G_{U\text{-}F}$ with surface area changes for different classes of mutations (single, double, and triple, Val→Ala, Phe→Leu, etc.), with potentially different interactions in the unfolded state.

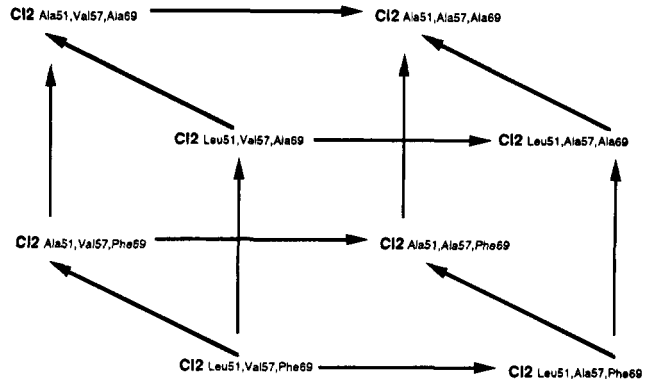

FIGURE 4: Triple mutant box for determining the third-order coupling between all three residues in the minicore of CI2.

Table 6: Higher-Order Interaction Energies in the Hydrophobic Minicore

triple mutant	$\Delta^3G_{int}^{U\text{-}F}$ (water) (kcal/mol)[a]	$\Delta\Delta G_{U\text{-}F}^{[G]50\%}$ (kcal/mol)
LA51/VA57/FL69	0.27 ± 0.16	3.48 ± 0.07
LV51/VA57/FL69	−0.05 ± 0.30	2.72 ± 0.05

[a] For triple mutant analysis of residues X, Y, and Z (Horovitz & Fersht, 1992), $\Delta^3G_{int}^{U\text{-}F} = \Delta\Delta G_{E\text{-}XYZ\rightarrow E}^{U\text{-}F} - \Delta\Delta G_{E\text{-}XYZ\rightarrow E\text{-}X}^{U\text{-}F} + \Delta\Delta G_{E\text{-}XYZ\rightarrow E\text{-}Y}^{U\text{-}F} + \Delta\Delta G_{E\text{-}XYZ\rightarrow E\text{-}Z}^{U\text{-}F} + \Delta\Delta G_{E\text{-}XYZ\rightarrow E\text{-}YZ}^{U\text{-}F} + \Delta\Delta G_{E\text{-}XYZ}^{U\text{-}F} + \Delta\Delta G_{E\text{-}XY\rightarrow E\text{-}XY}^{U\text{-}F}$.

We focus on two structural parameters, namely packing and solvent-accessible surface area. Protein interiors are packed very tightly (Richards, 1977; Chothia, 1975; Harpaz et al., 1994b) and thus maximize van der Waals' interactions as well as contributing to hydrophobic stabilization by exclusion of solvent. Mutations in the minicore and the major hydrophobic core of CI2 exhibit similar correlations between changes in stability and changes in exposed hydrophobic surface area, namely 59 and 55 cal/Å^2, respectively. For the minicore (but not the core), the correlation between changes in surface area and changes in stability is significantly improved by inclusion of a term for changes in exposed surface area of atoms that can make hydrogen bonds with solvent (the correlation coefficient for the linear fit between experimental and calculated values of $\Delta\Delta G_{U\text{-}F}$ improves from 0.71 to 0.95). The equation (eq 7) is similar to that obtained for Ala→Gly mutations in the two major helices of barnase (eq 8). The polar term ΔA_{HB} was originally introduced to rationalize the position dependence of the different α-helix propensities of Ala and Gly in barnase (Serrano et al., 1992b) but is also relevant to the minicore.

The packing density of the minicore, i.e. the number of methylene groups within a certain distance (6 Å) of each mutated side chain atom, is a crucial determinant of protein stability. The packing parameter n_C by itself more than adequately explains the structural basis for the loss in stability resulting from mutations ($\Delta\Delta G_{U\text{-}F}$), since there is an excellent correlation ($r = 0.995$ for 10 points) between $\Delta\Delta G_{U\text{-}F}$ and n_C. However, packing in the minicore, where all the side chain atoms are nonpolar, does not result entirely from nonpolar interactions. The correlation between $\Delta\Delta G_{U\text{-}F}$ and

packing density is only slightly reduced when all atoms, including polar atoms, within 6 Å of the atoms removed by mutation are included in the packing parameter.

The surface area factors by themselves provide good parameters that adequately describe the effect of mutation on stability, since ΔA_{HP} and ΔA_{HB} in combination correlate $\Delta\Delta G_{calculated}$, calculated from multiple linear regression, adequately with the measured values of $\Delta\Delta G_{U\text{-}F}$. Further, the nature of the correlation is similar to that of the exposed residues in the helices of barnase (where there is no correlation between $\Delta\Delta G_{U\text{-}F}$ and n_C). Yet, for the minicore, the best correlation is between $\Delta\Delta G_{U\text{-}F}$ and n_C. This apparent contradiction can be explained by the correlation between changes in surface area and packing density (eqs 10 and 11). Thus, for the partly exposed minicore, there is an interdependence of all three structural factors.

For other areas of CI2, such as the α-helix and the β-sheet, inclusion of the packing factor does not improve correlation between $\Delta\Delta G_{U\text{-}F}$ and $\Delta\Delta G_{calculated}$ (Otzen & Fersht, 1995; L. S. Itzhaki and A. R. Fersht, unpublished results), and changes in the stability of α-helices of barnase on mutation of Ala→Gly are fully accounted for by correlations with changes in surface area (Serrano et al., 1992b).

The effects of hydrophobic changes at the surface of the protein are consistent with the model of the hydrophobic effect as described by Kauzmann, in which stabilization is provided by the transfer of hydrocarbon surfaces from the solvent to the interior of the protein (Kauzmann, 1959). However, in the core, interactions are dominated by the van der Waals' term, since van der Waals' interactions are additive, and so the higher the packing density, the stronger the van der Waals' interactions. The interdependence of the three structural parameters n_C, ΔA_{HP}, and ΔA_{HB} in the minicore suggests that interactions in partly exposed parts of proteins are governed by a mixture of the classical hydrophobic effect and van der Waals' interactions.

ACKNOWLEDGMENT

We thank Y. Harpaz for supplying the program used to calculate changes in solvent-exposed surface area.

REFERENCES

Bode, W., & Huber R (1992) *Eur. J. Biochem. 204*, 433−451.
Chothia, C. (1975) *Nature 254*, 304−308.
Clarke, J., & Fersht, A. R. (1993) *Biochemistry 32*, 4322−4329.
Creighton, T. E., & Shortle, D. (1994) *J. Mol. Biol. 242*, 670−682.
Dill, K. A. (1990) *Biochemistry 29*, 7133−7155.
Eriksson, A. E., Baase, W. A., Zhang, X.-J., Heinz, D. W., Blaber, M., Baldwin, E. P., & Matthews, B. W. (1992) *Science 255*, 178−183.
Eriksson, A. E., Baase, W. A., & Matthews, B. W. (1993) *J. Mol. Biol. 229*, 747−769.
Fersht, A. R., & Serrano, L. (1993) *Curr. Opin. Struct. Biol. 3*, 75−83.
Fersht, A. R., Matouschek, A., & Serrano, L. (1992) *J. Mol. Biol. 224*, 771−782.
Harpaz, Y., el Masry, N., Fersht, A. R., & Henrick, K. (1994a) *Proc. Natl. Acad. Sci. U.S.A. 91*, 311−315.
Harpaz, Y., Gerstein, M., & Chothia, C. (1994b) *Structure 2*, 641−649.
Horovitz, A., & Fersht, A. R. (1992) *J. Mol. Biol. 224*, 733−740.
Innis, M. A., & Gelfand, D. H. (1990) in *PCR protocols: A guide to methods and applications* (Innis, M. A., Gelfand, D. H., Sninsky, J., & White, T. J., Eds.) pp 3−12, Academic Press, San Diego, CA.
Jackson, S. E., & Fersht, A. R. (1994) *Biochemistry 33*, 13880−13887.
Jackson, S. E., Moracci, M., el Masry, N., Johnson, C., & Fersht, A. R. (1993) *Biochemistry 32*, 11259−11269.
Jandu, S. K., Ray, S., Brooks, L., & Leatherbarrow, R. J. (1990) *Biochemistry 29*, 6264−6469.
Kauzmann, W. (1959) *Adv. Protein Chem. 14*, 1−63.
Kellis, J. T., Jr., Nyberg, K., Sali, D., & Fersht, A. R. (1988) *Nature 333*, 784−786.
Kellis, J. T., Jr., Nyberg, K., & Fersht, A. R. (1989) *Biochemistry 28*, 4914−4922.
Kim, K.-Y., Tao, F., Fuchs, J., Danishevsky, A. T., Housset, D., Wlodawer, A., & Woodward, C. (1993) *Protein Sci. 2*, 588−596.
Kraulis, P. J. (1991) *J. Appl. Crystallogr. 24*, 946−950.
Lim, W. A., Farruggio, D. C., & Sauer, R. T. (1992) *Biochemistry 31*, 4324−4333.
Longstaff, C., Campbell, A. F., & Fersht, A. R. (1990) *Biochemistry 29*, 7339−7347.
Ludvigsen, S., Shen, H., Kjær, M., Madsen, J. C., & Poulsen, F. M. (1991) *J. Mol. Biol. 222*, 621−635.
Matthews, B. W. (1993) *Annu. Rev. Biochem. 62*, 139−160.
McPhalen, C. A., & James, M. N. G. (1987) *Biochemistry 26*, 261−269.
McPhalen, C. A., Svendsen, I., Jonassen, I., & James, M. N. G. (1985) *Proc. Natl. Acad. Sci. U.S.A. 82*, 7242−7246.
Otzen, D. E., & Fersht, A. R. (1995) *Biochemistry 34*, 5718−5724.
Prevost, M., Wodak, S. J., Tidor, B., & Karplus, M. (1991) *Proc. Natl. Acad. Sci. U.S.A. 88*, 10880−10884.
Richards, F. M. (1977) *Annu. Rev. Biophys. Bioeng. 6*, 151−176.
Rose, G. D., & Roy, S. (1980) *Proc. Natl. Acad. Sci. U.S.A. 77*, 4643−4647.
Serrano, L., Kellis, J. T., Cann, P., Matouschek, A., & Fersht, A. R. (1992a) *J. Mol. Biol. 224*, 783−804.
Serrano, L., Neira, J. L., Sancho, J., & Fersht, A. R. (1992b) *Nature 356*, 453−455.
Shortle, D., Stites, W. E., & Meeker, A. K. (1990) *Biochemistry 29*, 8033−8041.
Svendsen, I., Boisen, S., & Hejgaard, J. (1982) *Carlsberg Res. Commun. 47*, 45−53.
Tanford, C. (1968) *Adv. Protein Chem. 23*, 121−282.
Tanford, C. (1973) *The Hydrophobic Effect*, Wiley & Sons, New York.
Varadarajan, R., & Richards, F. M. (1992) *Biochemistry 31*, 12315−12327.

BI951152N